Nonlocality in prior-form distorted-wave Born approximation

Jin Lei [1,2,*] and Zhongzhou Ren [1]

[1] *School of Physics Science and Engineering, Tongji University, Shanghai 200092, China*

[2] *Southern Center for Nuclear-Science Theory (SCNT), Institute of Modern Physics, Chinese Academy of Sciences, Huizhou 516000, Guangdong Province, China*

(Received 13 March 2026; revised 27 September 2026; accepted 30 September 2026; published 16 October 2026)

In the distorted wave Born approximation, the optical potentials of the entrance and exit channels are constrained by elastic scattering only on the energy shell, so their interior behavior, which a local Woods-Saxon form fixes by convention, is in fact left undetermined. We represent this off-shell freedom through the nonlocality of the optical potential and ask how far it propagates into reaction observables. A unitary transformation of the two-body Hamiltonian generates a continuous family of nonlocal potentials that are phase-shift equivalent, for every partial wave, to a given local potential, while differing in their interior wave functions. Applied to prior-form transfer and nonelastic breakup, the family produces a band of cross sections that share identical two-body elastic observables yet differ appreciably at forward angles. This nonlocality uncertainty is carried by the low partial waves that sample the nuclear interior and is suppressed by the Coulomb and centrifugal barriers, so it is largest for light, weakly charged systems and is expected to be small for heavy ones. The widely used Perey-Buck prescription is not a member of this family. Its nonlocality range is a parameter fitted under the assumption that one energy-independent nonlocal potential serves every energy; freed from that assumption, the range generates a second family that reshapes the interior differently. The off-shell freedom is therefore wider than either family alone maps.

DOI: 10.1103/8lpg-kcff

I. INTRODUCTION

The distorted wave Born approximation (DWBA) is the standard tool for analyzing transfer and breakup reactions, through which much of our knowledge of single-particle structure away from stability is extracted [1]. Its central simplification is to replace the many-body projectile-target interaction by an optical potential, the parameters of which are adjusted to reproduce elastic scattering. Elastic scattering, however, determines the potential only through its asymptotic phase shifts, that is, on the energy shell. The customary choice of a local Woods-Saxon form is a convention that silently fixes the interior, off-shell behavior of the interaction. Potentials that share the same phase shifts but differ in the interior, the long-recognized inverse-scattering ambiguity [2], are indistinguishable in elastic scattering yet act differently on any observable that samples the interior of the scattering wave function, as transfer and nonelastic breakup (NEB) amplitudes do. How large this ambiguity is in reaction observables is the subject of this work.

The natural language for this freedom is the nonlocality of the optical potential. Eliminating the nonelastic channels from the many-body problem leaves an effective interaction that is nonlocal in the projectile coordinate, describing a process that leaves the elastic channel at one point and returns to it at another [3,4]. Perey and Buck modeled this by a nonlocal form with a Gaussian dependence on the nonlocality distance and introduced its energy-dependent local equivalent [5]; the correspondence between the two was refined by Perey and Saxon [6] and by Frahn [7] to leading order in the nonlocality range, and cast in closed, wave-function-independent form by Fiedeldey [8]. This line of work establishes a one-to-one mapping from a given nonlocal potential to its local equivalent, faithful within the accuracy of the reduction. For a fixed range it yields a single nonlocal potential, not a family, and so does not by itself expose the off-shell freedom as a controlled variation.

A construction that does generate families of phase-equivalent nonlocal potentials is the separable representation of the optical potential [9–11], in which a local potential is replaced by a finite-rank interaction that reproduces the elastic S matrix at a chosen set of support energies. The induced nonlocality is found to follow the Perey-Buck Gaussian only near the interior, departing from it in the surface region and growing with angular momentum [11]. What has been missing is a controlled, exactly phase-equivalent family, built directly in coordinate space and immediately usable in the DWBA, with which the off-shell freedom of a fitted optical potential can be turned into a band of reaction observables.

In this work we construct such a family. A unitary transformation of the two-body Hamiltonian maps a local optical potential into a one-parameter family of nonlocal potentials that are exactly phase-shift equivalent, for all partial waves, while their interior wave functions vary continuously. Applying the family to the prior-form DWBA, we quantify the

*Contact author: jinl@tongji.edu.cn

 ©2026 American Physical Society

nonlocality uncertainty in the transfer reaction ^{16}O$(d, p)\,^{17}$O and in the nonelastic breakup ^{93}Nb(d, pX). We find that the uncertainty is appreciable at forward angles, that it is carried almost entirely by the low partial waves that probe the nuclear interior, and that it is screened by the Coulomb and centrifugal barriers, so that it grows for light, weakly charged systems and is expected to be small for heavy ones. Because elastic data cannot constrain the off-shell freedom, this uncertainty is an irreducible contribution to the DWBA uncertainty, here made explicit and quantified, and it bears directly on the extraction of spectroscopic information.

II. THEORETICAL FRAMEWORK

We consider a two-body projectile $a\ (=b+x)$ incident on a target A, with the fragment b detected,

$$a(=b+x)+A \to b+B^*, \tag{1}$$

where B^* denotes any state of the $x+A$ system. A bound $x+A$ subsystem corresponds to transfer, while a positive x–A relative energy corresponds to breakup. Breakup splits into elastic breakup, in which A remains in its ground state, and the nonelastic breakup (NEB) that collects all other final states; the latter is dominated by transfer to the continuum [12]. We treat transfer and NEB on the same footing. The three-body Hamiltonian is

$$H = T + V_{bx} + U_{bA} + U_{xA}, \tag{2}$$

where T is the kinetic energy operator, V_{bx} is the real interaction binding the projectile, and U_{bA}, U_{xA} are the fragment-target optical potentials; for transfer the bound x–A system is described by a real binding interaction, $U_{xA} \to V_{xA}$. The exact solution would follow from the Faddeev equations [13] or, after expansion on $b+x$ states, from the continuum-discretized coupled channels [14]; in practice the DWBA remains the standard working approximation. For transfer to a definite bound state the post form is the common choice, whereas NEB is naturally formulated in the prior form; we use the prior form for both so that the two reactions are treated on the same footing, and verify the post-prior consistency of the transfer case below. There the model Hamiltonian reads

$$H^{\mathrm{DWBA}} = T + U_{bB^*} + U_{xA} \tag{3}$$

with U_{bB^*} taken to approximate $V_{bx}+U_{bA}$ and fitted, in a local Woods-Saxon form, to $b+B^*$ elastic scattering. Attempts to derive U_{bB^*} microscopically are advancing [15–18], but the phenomenological local potential remains the standard input, and it is its off-shell ambiguity that concerns us.

The usual way to bring nonlocality into the DWBA is the Perey-Buck prescription [5,19], in which the local potential is replaced by

$$U^{\mathrm{PB}}(\vec{r},\vec{r}\,') = U^{\mathrm{NL}}\!\left(\frac{1}{2}|\vec{r}+\vec{r}\,'|\right)G_\beta(|\vec{r}-\vec{r}\,'|),$$
$$G_\beta(s) = \frac{1}{\pi^{3/2}\beta^3}\,e^{-s^2/\beta^2}, \tag{4}$$

where U^{NL} has the radial form of a local optical potential, a real Woods-Saxon volume term and an imaginary surface term, and G_β is a normalized Gaussian of range β, so that U^{PB} reduces to the local potential $U^{\mathrm{NL}}(r)\,\delta(\vec{r}-\vec{r}\,')$ as $\beta \to 0$. Perey and Buck fitted an energy-independent U^{NL} with $\beta = 0.85$ fm to neutron scattering [5]. At center-of-mass energy E the nonlocal potential has an energy-dependent local equivalent U_L, fixed to leading order in β by $U_L(r)\exp[\mu\beta^2(E-U_L(r))/2\hbar^2] = U^{\mathrm{NL}}(r)$, and inside the nucleus the nonlocal wave function is reduced relative to the local one by the Perey damping factor [8]. For a given β this construction yields one nonlocal potential.

To expose the ambiguity as a controlled variation, rather than through this single prescription, we transform the effective two-body Hamiltonian of the $b+B^*$ system, $H_{2b} = h_0 + U$, with h_0 the kinetic energy and U the fitted local potential. Following Refs. [20,21] we define

$$\tilde{H}_{2b} = \mathcal{U}H_{2b}\mathcal{U}^\dagger = h_0 + \tilde{U}, \tag{5}$$

where the operator

$$\mathcal{U} = 1 - 2|h\rangle\langle h| \tag{6}$$

is both unitary and Hermitian, a reflection in the state $|h\rangle$, provided $\langle h|h\rangle = 1$. Following Ref. [22] we take, in each partial wave ℓ,

$$h_\ell(r) = \langle r\ell \mid h\rangle = N r^\ell e^{-br^2} \tag{7}$$

with N fixed by normalization and b a free parameter that sets the radial scale of the generator, not to be confused with the detected fragment b introduced above. The transformed potential is

$$\begin{aligned}\langle r\ell|\tilde{U}|r'\ell\rangle = {}& \frac{U(r)}{rr'}\delta(r-r') - 2\langle r\ell \mid h\rangle\langle h|h_0+U|r'\ell\rangle \\ & - 2\langle r\ell|h_0+U|h\rangle\langle h \mid r'\ell\rangle \\ & + 4\langle r\ell \mid h\rangle\langle h|h_0+U|h\rangle\langle h \mid r'\ell\rangle\end{aligned} \tag{8}$$

with

$$\begin{aligned}&2\langle r\ell|h_0+U|h\rangle\langle h \mid r'\ell\rangle \\ &\quad = 2h_\ell(r')\left[-\frac{\hbar^2}{2\mu}\left(\frac{1}{r}\frac{d^2}{dr^2}r - \frac{\ell(\ell+1)}{r^2}\right) + U(r)\right]h_\ell(r)\end{aligned} \tag{9}$$

and

$$\begin{aligned}&4\langle r\ell \mid h\rangle\langle h|h_0+U|h\rangle\langle h \mid r'\ell\rangle \\ &\quad = 4h_\ell(r)h_\ell(r')\int_0^\infty r''^2 h_\ell(r'')\left[-\frac{\hbar^2}{2\mu}\left(\frac{1}{r''}\frac{d^2}{dr''^2}r'' \right.\right. \\ &\qquad \left.\left. - \frac{\ell(\ell+1)}{r''^2}\right) + U(r'')\right]h_\ell(r'')\,dr''.\end{aligned} \tag{10}$$

In Eqs. (9) and (10) the two-body kinetic energy operator h_0 acts on the generator standing immediately to its right. The transformed potential $\tilde{U}$ is nonlocal and partial-wave dependent. The operator $\mathcal{U}$ is exactly unitary, so it preserves the spectrum of H_{2b}; whether it also preserves the phase shifts

depends on its action in the asymptotic region. Because $h_\ell(r)$ falls off as a Gaussian, it is confined to the interior for all but the smallest b, and is negligible beyond the matching radius at which the wave function joins its asymptotic form. The transformed potential then differs from U only in the interior and leaves the asymptotic region untouched, so the scattering state computed with $\tilde{U}$ has the same phase shift, and the same S matrix, as that computed with U, for every partial wave. Although the generator peaks at a larger radius as the angular momentum increases, $r_{\rm peak} = \sqrt{\ell/2b}$, it remains well inside the matching radius for the values of b used here. In the calculations reported here the elastic S matrix is preserved to better than nine significant figures over the range $0.2 \leqslant b \leqslant 6.0$ fm^{-2} used below, for every partial wave up to $\ell = 5$, so the equivalence is numerically exact and carries no expansion parameter; it is spoiled only for long-range generators, where b is so small that the Gaussian tail reaches the matching radius (for $\ell = 0$ here, $b \lesssim 0.06$ fm^{-2}), a limit of the finite radial box rather than of the transformation. The free parameter b controls the radial scale on which the interior is reshaped: a small b gives a long-range nonlocality, a large b a short-range one concentrated deep inside. Varying b within this window thus sweeps a continuous family of phase-equivalent potentials whose only difference is the off-shell, interior content of the wave function. Any comparison with the Perey-Buck construction has to be made partial wave by partial wave, since the radial form of the Perey-Buck potential is itself ℓ dependent through the projection $\int d(\cos\theta)\, U\, P_\ell(\cos\theta)$; we carry out such a comparison below.

The transfer and NEB cross sections are evaluated from the prior-form T matrix. To isolate the nonlocality of a single channel, we apply the transformation only to the potential U_{bB^*} that generates the $b + B^*$ scattering state and keep all other interactions local.

III. NUMERICAL RESULTS

We first illustrate the structure of the transformed potential for $p + {}^{17}$O at 17 MeV, representative of the exit channel of the ^{16}O$(d, p)^{17}$O reaction studied below, using a systematic potential fitted to nucleon elastic scattering from $1p$-shell nuclei [23]. Figure 1 shows the real part of the nonlocal part of the s-wave potential for several values of b. For $b = 0.1$ fm^{-2} the off-diagonal range exceeds the nuclear size, $r_0(A_p^{1/3} + A_T^{1/3}) \approx 4.29$ fm with $r_0 = 1.2$ fm, while increasing b confines the nonlocality to a progressively smaller region inside the Coulomb barrier. The transformation therefore reshapes the interaction precisely where elastic scattering has no resolving power.

The scattering wave functions of the nonlocal potentials, obtained with the Lagrange-mesh R-matrix method [24,25], are shown in Fig. 2 for $\ell = 0, 2, 5, 10$. The asymptotic parts of the local and transformed wave functions coincide, as the exact phase equivalence requires, while their interior parts differ. The longest-range case, $b = 0.1$ fm^{-2}, has a nonlocality reaching beyond the nuclear surface and pushes the interior outward; we discard it as unphysical and keep $b \gtrsim 0.2$ fm^{-2} below. The lowest partial waves set this bound, since only their wave functions reach the interior. For higher ℓ the

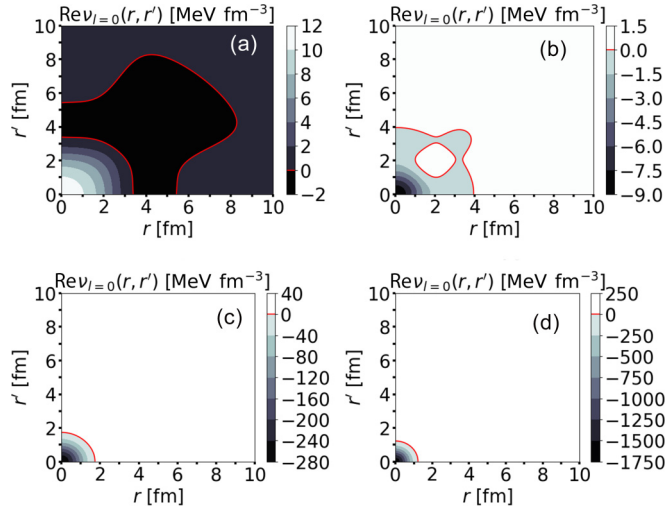


FIG. 1. Contour plots of the real part of the nonlocal part of the transformed $p + {}^{17}$O s-wave potential for (a) $b = 0.1$ fm^{-2}, (b) $b = 0.2$ fm^{-2}, (c) $b = 0.5$ fm^{-2}, and (d) $b = 1.0$ fm^{-2}.

generator peaks farther out, at $r_{\rm peak} = \sqrt{\ell/2b}$, but the centrifugal barrier removes the wave function from that region, so the same bound is conservative for all ℓ and for the systems considered here. Because it is set by the radial extent of the generator relative to the nuclear surface, the bound applies at the exit-channel energy of the transfer calculation below as well as at the 17 MeV used here.

How the interior is reshaped is fixed by the transformation itself. With χ the scattering state of the local potential at energy E in the same partial wave, $\tilde{H}_{2b}(\mathcal{U}\chi) = \mathcal{U}H_{2b}\mathcal{U}^\dagger\mathcal{U}\chi = E\,\mathcal{U}\chi$, and $\mathcal{U}\chi$ keeps the asymptotic form of χ because the generator is confined to the interior. It is, therefore, the scattering state of the transformed Hamiltonian at the same energy and carries the same normalization. The reduced radial functions of Fig. 2, $u_\ell = r\chi_\ell$ for the local potential and $r(\mathcal{U}\chi)_\ell$ for the transformed one, therefore, obey

$$u_b(r) - u(r) = -2\, r\, h_\ell(r)\, \langle h \mid \chi \rangle, \tag{11}$$

where u is the local result and u_b the transformed one for a given value of the family parameter b, the partial-wave label being suppressed on both. The difference is a single peak of shape $r^{\ell+1}e^{-br^2}$ at $\sqrt{(\ell+1)/2b}$ with an amplitude set by the overlap $\langle h|\chi\rangle$. The radial extent of the reshaped region therefore shrinks monotonically as b grows, but its amplitude need not, and in the s wave it does not: the long-range generators span several oscillations of u, so the overlap largely cancels and the $b = 0.1$ and 0.2 fm^{-2} curves stay close to the local one, whereas the short-range generators sit in a narrow interior region where no such cancellation occurs. What survives in a reaction amplitude is not the height of that difference but its overlap with the transition source, and that overlap inherits the same nonmonotonic behavior, as the cross-section bands below will show. The interior difference is also progressively quenched as ℓ grows, being sizable for $\ell = 0, 2$, small already for $\ell = 5$ over the retained range $b \gtrsim 0.2$ fm^{-2}, and negligible by $\ell = 10$, because the centrifugal barrier excludes the wave function from the region in which the transformation acts. The

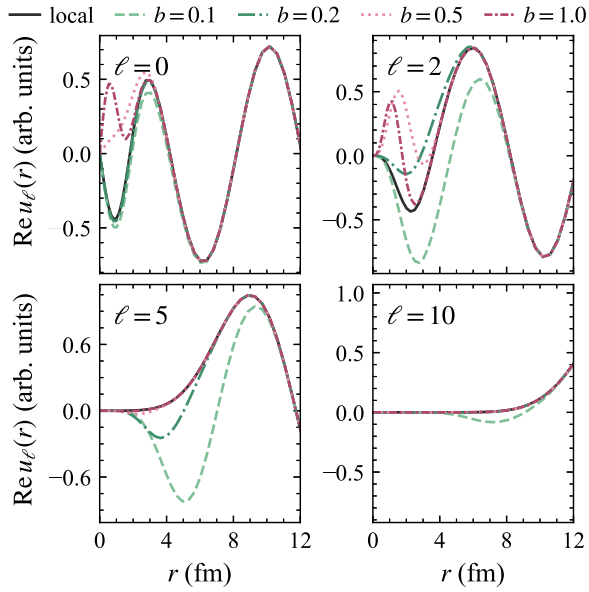


FIG. 2. Real part of the reduced radial $p + {}^{17}\mathrm{O}$ scattering wave function, $u_\ell = r\chi_\ell$, from phase-shift-equivalent local and nonlocal potentials, for $\ell = 0, 2, 5, 10$. In each panel the solid line is the local result and the remaining curves, drawn light to dark with increasing b, are the results for the unitary-transformed nonlocal potentials with $b = 0.1, 0.2, 0.5, 1.0$ fm^{-2}. Each differs from the local result by the single peak of Eq. (11), which moves inward as b grows while its amplitude follows the overlap $\langle h|\chi\rangle$ and is therefore not ordered in b; in the s wave that overlap nearly cancels at $b = 0.2$ fm^{-2}. The interior difference is large for $\ell = 0, 2$, already small for $\ell = 5$ once the discarded $b = 0.1$ fm^{-2} case is set aside, and negligible by $\ell = 10$, where the centrifugal barrier excludes the wave function from the region in which the transformation acts.

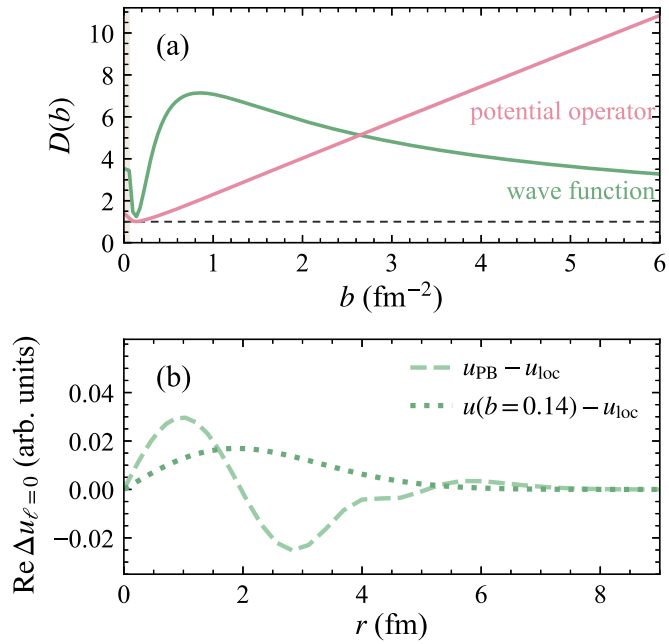


FIG. 3. Recovery test for a Perey-Buck potential ($n + {}^{40}\mathrm{Ca}$, $\beta = 0.85$ fm, $E_n = 10$ MeV): the transformation is applied to the Fiedeldey local equivalent and b is scanned. (a) Distances D_u (wave function) and D_U (potential operator) of Eq. (12); the dashed line at unity marks a transformation that has brought the local equivalent no closer to the Perey-Buck input than it began. Both panels are for $\ell = 0$. (b) The interior distortion each construction produces, measured from the local equivalent: the Perey damping multiplies the wave function and so oscillates with it, whereas the closest member of the family, at $b = 0.14$ fm^{-2}, adds a single peak.

off-shell freedom thus lives in the interior and is accessible only to the low partial waves, a localization that reappears at the cross-section level in Fig. 6.

The same construction answers whether a member of the family can reproduce a Perey-Buck potential. We start from the local equivalent U_{loc} of the Perey-Buck potential of Eq. (4) for $n + {}^{40}\mathrm{Ca}$ at 10 MeV with the original parameters and $\beta = 0.85$ fm [5], built following Fiedeldey [8], who adds next-order corrections to the leading-order U_L defined below Eq. (4). In the form used there the Perey-Buck interior is obtained by dividing the local wave function by $f(r) = \exp[-\frac{1}{8}\beta^2 U_L^0(r)]$, where U_L^0 is the nuclear part of the leading-order U_L scaled by $2\mu/\hbar^2$; since U_L^0 is attractive, $|f| > 1$ inside the nucleus and $1/f$ is the Perey damping factor. The local Coulomb term is common to every member and is left out. We then apply the transformation and scan b. Phase equivalence holds over the range used here and, at the fixed matching radius, fails only at its long-range edge, first in the higher partial waves, whose generators peak farther out: at $b = 0.06$ fm^{-2} the s wave is still equivalent and the higher ones are not. Closeness to the Perey-Buck input is measured by

$$D_u(b) = \frac{\|u_b - u_{\mathrm{PB}}\|}{\|u_{\mathrm{loc}} - u_{\mathrm{PB}}\|}, \quad D_U(b) = \frac{\|\tilde{U}_b - U_{\mathrm{PB}}\|_{\mathrm{off}}}{\|U_{\mathrm{loc}} - U_{\mathrm{PB}}\|_{\mathrm{off}}}, \quad (12)$$

where u_{loc} is the reduced radial wave function of the local equivalent, u_b that of the transformed potential $\tilde{U}_b$, and $u_{\mathrm{PB}} = u_{\mathrm{loc}}/f$ the Perey-damped one that stands for the Perey-Buck interior; U_{PB} is the exact $\ell = 0$ projection of the kernel of Eq. (4). Each norm is the square root of the integrated squared modulus of the difference, over r for the wave functions and over r and r' for the kernels, in the same reduced radial representation; for D_U the diagonal $r = r'$, which carries the local part, is omitted. The denominators are the distances of the untransformed local equivalent from the Perey-Buck input, so zero would mean exact recovery and unity no improvement on the starting point.

No member of the family recovers the Perey-Buck potential: neither distance falls below unity, as Fig. 3(a) shows. The wave function comes closest at $D_u = 1.24$, near $b \approx 0.14$ fm^{-2}, and the operator never comes nearer than about one percent above unity, a margin that does not shrink on a finer radial mesh. Figure 3(b) shows why. The Perey damping multiplies the local wave function and so oscillates with it, whereas the transformation adds a single peak, and no choice of b matches the two. For the operator the obstruction is structural rather than one of magnitude: the unitary nonlocality has finite rank, the Perey-Buck kernel is smooth and of full rank, and the two cannot coincide. At closest approach the unitary nonlocality is about one seventh of the Perey-Buck one; the short-range members are stronger but confined to a region the

Perey-Buck kernel barely reaches. The operator distance is computed for $\ell = 0$, the partial wave in which the Perey-Buck kernel is projected here. The wave-function scan, extended to $\ell \leqslant 5$, gives the same answer. The s wave 1.24 is the only true minimum; for $\ell \geqslant 1$ the distance approaches unity from above at the short-range end of the scan, where the centrifugal barrier keeps the wave function out of the region in which the transformation acts, so the overlap in Eq. (11) vanishes and u_b returns to $u_{\rm loc}$. Separable-representation analyses reach the same conclusion from the opposite side [11].

The Perey-Buck construction can nonetheless be read as a family in its own right. The value $\beta = 0.85$ fm is not fundamental: it is one of the parameters Perey and Buck fitted to neutron elastic scattering on lead at 7 and 14.5 MeV, under the assumption that a single energy-independent nonlocal potential serves every energy [5]. That the resulting potential then reproduces the empirical energy dependence of the local one is a result of the model, not the constraint that fixed the range. Once the assumption is dropped and the nonlocal potential is allowed to be energy dependent, the range becomes free, and at a fixed local potential the factor $f(r;\beta)$ labels a family of nonlocal potentials that share one local equivalent, hence one set of phase shifts, and differ in the interior. Two things separate it from the family used here. The equivalence holds only to the accuracy of the local-equivalent mapping, an expansion whose size is set by $\beta^2|U|/4c$ with $c = \hbar^2/2\mu$; that parameter is 0.24 at $\beta = 0.6$ fm and 0.95 at $\beta = 1.2$ fm, so the further the range is opened the less controlled the equivalence becomes, whereas the unitary family is phase equivalent by construction and to numerical precision. And the two reshape the interior differently: the Perey factor damps the whole interior smoothly and multiplicatively, while the transformation adds the single peak of Eq. (11) at a radius selected by b. For the $p + {}^{17}$O exit channel used below, estimating the interior wave function with the Perey damping factor rather than by solving the nonlocal equation, moving β from 0.6 to 1.2 fm changes the s-wave interior by 6.5% to 22% of the peak wave function, the same order as the weakest members of the unitary band. Neither family exhausts the off-shell freedom; each is one direction in it, so the bands reported below are an envelope taken along one direction and not over the whole of that freedom, which can only be wider.

We now apply the family to reactions, beginning with the transfer ${}^{16}\mathrm{O}(d,p){}^{17}\mathrm{O}_{g.s.}$. The prior-form cross section is

$$\frac{d\sigma}{d\Omega} = \frac{\mu_{\rm out}\,\mu_{\rm in}}{(2\pi\hbar^2)^2}\frac{k_{\rm out}}{k_{\rm in}}|\langle\chi^{(-)}_{p-{}^{17}\mathrm{O}}\phi_{n-{}^{16}\mathrm{O}}|V_{\rm prior}\,|\chi^{(+)}_{d-{}^{16}\mathrm{O}}\phi_{np}\rangle|^2 \tag{13}$$

with μ the reduced masses, k the wave numbers, χ the distorted waves, ϕ the bound states, and $V_{\rm prior} = V_{n-{}^{16}\mathrm{O}} + U_{p-{}^{16}\mathrm{O}} - U_{d-{}^{16}\mathrm{O}}$. The exit-channel distorted wave $\chi^{(-)}_{p-{}^{17}\mathrm{O}}$ is generated by the fitted optical potential, the off-shell ambiguity of which we now propagate through the transformation; the elastic observables are unchanged while the interior of $\chi^{(-)}$ varies. The magnitude of the effect is set by the weight of the nuclear interior in the transition amplitude. Whether ${}^{16}\mathrm{O}(d,p){}^{17}\mathrm{O}$ is peripheral is model dependent [26–28]: including deuteron breakup through the adiabatic or coupled-channels treatment suppresses the interior contribution, whereas at the DWBA level it remains appreciable [19], a conclusion supported by our quantum-mechanical test of the surface approximation in deuteron-induced reactions [29]. The present study therefore probes the regime in which nonlocality is expected to matter.

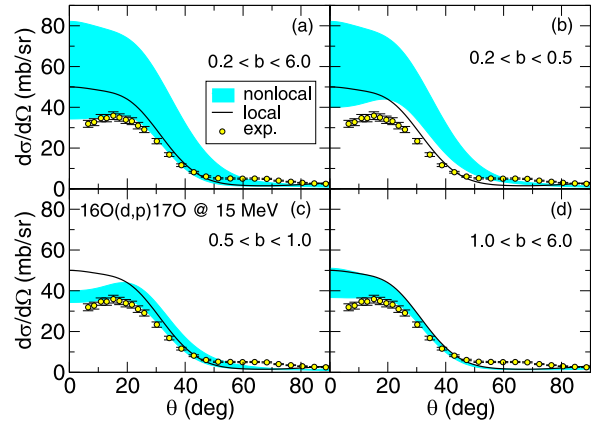


FIG. 4. Differential cross section of ${}^{16}\mathrm{O}(d,p){}^{17}\mathrm{O}$ at $E_d = 15$ MeV. The solid line is the DWBA result with the local potential of Ref. [30]; the shaded bands are the unitary-transformed nonlocal potentials for b between (a) 0.2 and 6.0, (b) 0.2 and 0.5, (c) 0.5 and 1.0, and (d) 1.0 and 6.0 fm^{-2}. Data are from Ref. [30].

Figure 4 shows the differential cross section at 15 MeV, with the local potential taken from Ref. [30]. The shaded bands collect the results of the nonlocal family over ranges of b. The normalization of the local calculation to the data is the usual spectroscopic factor, which links the measured cross section to the ${}^{16}\mathrm{O}+n$ single-particle content of ${}^{17}\mathrm{O}_{g.s.}$. The nonlocal band shows that this extraction carries an additional, irreducible uncertainty: potentials with identical elastic observables yield transfer cross sections that differ at forward angles. The deviation from the local result does not fall off monotonically with b, for the same reason the interior wave function does not. At 0° the longest-range members raise the cross section well above the local calculation, band and local calculation cross between $b = 0.2$ and 0.5 fm^{-2}, the deepest suppression is reached inside the interval $0.5 \leqslant b \leqslant 1.0$ fm^{-2}, and the result then turns back towards the local one as the reshaped region shrinks into the origin and stops overlapping the transition source. The width of each band therefore reflects the interval of b it covers and not a monotonic trend: of the three subintervals the widest is panel (b), the one that straddles the crossing.

For a ground-state transfer the post form is also available, and the two forms must give the same cross section. With the local exit potential, the post-form result, computed with the same numerical treatment, agrees with the prior form to 0.7% in the angle-integrated cross section (prior 183.9 mb, post 185.2 mb) and to within about 1% differentially across the angular range, rising to a few percent only at the most forward angles. This agreement, at the level expected from the finite-range remnant term, shows that the prior-form sensitivity to the interior is not an artifact of the representation, so the nonlocality effect is a genuine feature of the DWBA amplitude.

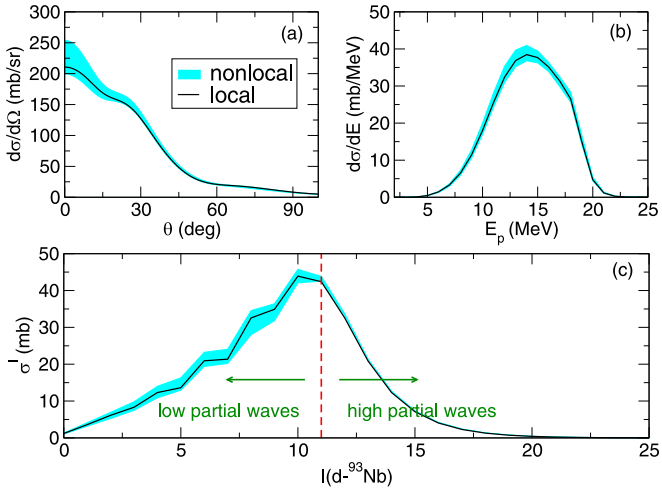


FIG. 5. Nonelastic breakup ^{93}Nb(d, pX) at 25.5 MeV. Solid line: local potential; shaded band: nonlocal family. (a) Proton angular distribution. (b) Proton energy distribution. (c) Cross section versus the projectile-target partial wave.

As a second and more demanding example, we consider the nonelastic breakup ^{93}Nb(d, pX), in which only the proton is detected, analyzed earlier in Ref. [31]. Schematically,

$$d + {}^{93}\mathrm{Nb} \to p + ({}^{93}\mathrm{Nb} + n)^*, \tag{14}$$

where $()^*$ denotes any ^{93}Nb $+n$ state other than the elastic-breakup one. Within the model of Ichimura, Austern, and Vincent [32] the NEB cross section is

$$\left.\frac{d^2\sigma}{dE_p d\Omega_p}\right|_{\mathrm{NEB}} = -\frac{2}{\hbar v_d}\rho_p(E_p)\langle\varphi_n(\vec{k}_p)|\,\mathrm{Im}[U_n]|\varphi_n(\vec{k}_p)\rangle \tag{15}$$

with ρ_p the proton density of states, v_d the deuteron velocity, U_n the $n +$ ^{93}Nb optical potential, and φ_n the n–^{93}Nb relative wave function for a proton scattered with momentum $\vec{k}_p$. The latter is

$$\varphi_n(\vec{k}_p, \vec{r}_n) = \varphi_n^{\mathrm{HM}}(\vec{k}_p, \vec{r}_n) + \varphi_n^{\mathrm{UT}}(\vec{k}_p, \vec{r}_n), \tag{16}$$

the Hussein-McVoy term [33]

$$\varphi_n^{\mathrm{HM}}(\vec{k}_p, \vec{r}_n) = \langle \vec{r}_n \chi_p^{(-)}|\chi_d^{(+)}\phi_{np}\rangle, \tag{17}$$

plus the Udagawa-Tamura term [34] from

$$(E_n - T_n - U_n)\varphi_n^{\mathrm{UT}}(\vec{k}_p, \vec{r}_n) = \langle \vec{r}_n \chi_p^{(-)}|V_{\mathrm{prior}}\,|\chi_d^{(+)}\phi_{np}\rangle. \tag{18}$$

We apply the transformation to the exit-channel p-^{94}Nb potential that generates $\chi_p^{(-)}$, using the parameters of Ref. [31] at 25.5 MeV.

The NEB results are shown in Fig. 5 with b varied over the same physical range $0.2 \leqslant b \leqslant 6.0$ fm^{-2}. The angular distribution in panel (a) shows that local and nonlocal potentials agree at large angles but that the nonlocal family opens a sizable band at forward angles. The partial-wave decomposition in panel (c) locates the effect: the whole band is carried by the low partial waves and has vanished by $L \approx 14$ with L the projectile-target orbital angular momentum, consistent with a band seen at forward angles and not at large ones. The energy distribution in panel (b) keeps its bell shape, the uncertainty concentrating near the peak. The same interior, low-partial-wave localization seen in the transfer reaction thus controls the NEB.

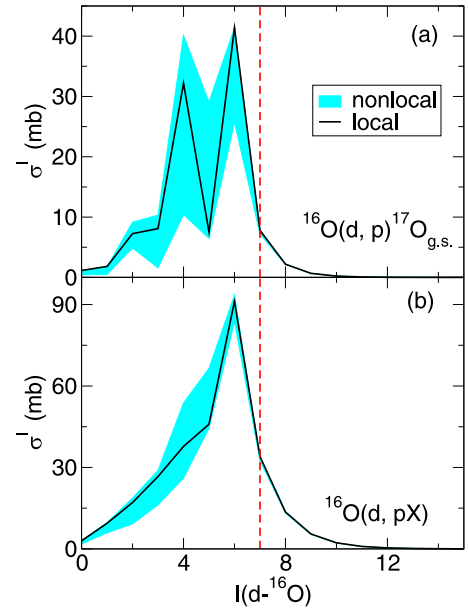


FIG. 6. Partial-wave distribution of the cross section for $d + {}^{16}$O at 15 MeV. (a) Transfer ^{16}O$(d, p)\,^{17}$O$_{g.s.}$. (b) Nonelastic breakup ^{16}O(d, pX).

To compare the two reaction mechanisms on a common footing, Fig. 6 shows the partial-wave distribution of the cross section for $d + {}^{16}$O at 15 MeV, the NEB computed with the KD02 potential [35] for $n + {}^{16}$O. The nonlocal effect is largest in the lowest partial waves and somewhat stronger for transfer than for NEB, and it disappears as the partial wave increases, where the local and nonlocal results coincide. This common behavior identifies the centrifugal and Coulomb barriers as the agents that screen the interior off-shell freedom: the higher the barrier, the smaller the interior weight, and the smaller the nonlocality uncertainty. The same barrier control of the interior weight appeared, across a range of systems and energies, in our quantum-mechanical study of the surface approximation for reactions induced by weakly bound nuclei [29]. It follows that the effect is largest for light, weakly charged systems at low energy and becomes negligible for heavy, strongly charged ones, a trend that should guide where nonlocality is included in the analysis of transfer and breakup data.

IV. SUMMARY AND CONCLUSIONS

We have shown that the off-shell freedom left undetermined by elastic scattering, the inverse-scattering ambiguity of a fitted optical potential, propagates into prior-form DWBA observables as a genuine uncertainty. To map this freedom in a controlled way, we introduced a unitary transformation that turns a local optical potential into a continuous family of nonlocal potentials, phase-shift equivalent for all partial waves, differing only in the interior of the wave function. A direct test shows that the Gaussian nonlocality of Perey-Buck is not a member of that family and that, for every partial wave

tested, no member of it comes closer to Perey-Buck than the local potential one starts from; the two constructions are complementary, one a one-to-one local-nonlocal map, the other a one-to-many phase-equivalent family. Freeing the Perey-Buck nonlocality range yields a second family, so the off-shell freedom is wider than the band mapped here. Applied to the transfer reaction $^{16}\mathrm{O}(d, p)\,^{17}\mathrm{O}$ and the nonelastic breakup $^{93}\mathrm{Nb}(d, pX)$, the family produces cross-section bands that share identical two-body elastic observables yet differ at forward angles, with the uncertainty carried almost entirely by the low partial waves that sample the interior and screened by the Coulomb and centrifugal barriers.

Because elastic data cannot constrain the off-shell content of the optical potential, this nonlocality is an irreducible contribution to the DWBA uncertainty in the spectroscopic information extracted from transfer and breakup; it matters for the light, weakly charged, low-energy systems that dominate studies far from stability, while the barrier screening leads us to expect it to be small for heavy, strongly charged targets. The magnitude of the bands is itself reaction-model dependent: treatments that suppress the interior weight, such as the adiabatic approximation or the continuum-discretized coupled channels, are expected to narrow them, a quantification we leave to future work. Reducing the uncertainty itself will require interactions whose off-shell content is fixed by more fundamental input.

ACKNOWLEDGMENT

This work was supported by the National Natural Science Foundation of China (Grants No. 12475132 and No. 12535009) and the Fundamental Research Funds for the Central Universities.

DATA AVAILABILITY

The data that support the findings of this article are not publicly available. The data are available from the authors upon reasonable request.

[1] N. K. Timofeyuk and R. C. Johnson, Theory of deuteron stripping and pick-up reactions for nuclear structure studies, Prog. Part. Nucl. Phys. **111**, 103738 (2020).
[2] K. Chadan, P. C. Sabatier, and R. G. Newton, *Inverse Problems in Quantum Scattering Theory*, 2nd ed., Theoretical and Mathematical Physics (Springer, Berlin/Heidelberg, 1989).
[3] H. Feshbach, Unified theory of nuclear reactions, Ann. Phys. **5**, 357 (1958).
[4] H. Feshbach, A unified theory of nuclear reactions. II, Ann. Phys. **19**, 287 (1962).
[5] F. Perey and B. Buck, A non-local potential model for the scattering of neutrons by nuclei, Nucl. Phys. **32**, 353 (1962).
[6] F. G. Perey and D. S. Saxon, The local energy approximation to nonlocality and finite range effects, Phys. Lett. **10**, 107 (1964).
[7] W. E. Frahn, Note on approximations to non-local nuclear interaction, Nucl. Phys. **66**, 358 (1965).
[8] H. Fiedeldey, The equivalent local potential and the Perey effect, Nucl. Phys. **77**, 149 (1966).
[9] D. J. Ernst, C. M. Shakin, and R. M. Thaler, Separable representations of two-body interactions, Phys. Rev. C **8**, 46 (1973).
[10] L. Hlophe, C. Elster, R. C. Johnson, N. J. Upadhyay, F. M. Nunes, G. Arbanas, V. Eremenko, J. E. Escher, and I. J. Thompson, Separable representation of phenomenological optical potentials of Woods-Saxon type, Phys. Rev. C **88**, 064608 (2013).
[11] M. Quinonez, L. Hlophe, and F. M. Nunes, Properties of a separable representation of optical potentials, Phys. Rev. C **102**, 024606 (2020).
[12] J. Lei and A. M. Moro, Unraveling the reaction mechanisms leading to partial fusion of weakly bound nuclei, Phys. Rev. Lett. **123**, 232501 (2019).
[13] L. D. Faddeev, Scattering theory for a three-particle system, Zh. Eksp. Teor. Fiz. **39**, 1459 (1960) [Sov. Phys. JETP **12**, 1014 (1961)].
[14] N. Austern, Y. Iseri, M. Kamimura, M. Kawai, G. Rawitscher, and M. Yahiro, Continuum-discretized coupled-channels calculations for three-body models of deuteron-nucleus reactions, Phys. Rep. **154**, 125 (1987).
[15] M. Burrows, R. B. Baker, C. Elster, S. P. Weppner, K. D. Launey, P. Maris, and G. Popa, *Ab initio* leading order effective potentials for elastic nucleon-nucleus scattering, Phys. Rev. C **102**, 034606 (2020).
[16] A. Idini, C. Barbieri, and P. Navrátil, *Ab initio* optical potentials and nucleon scattering on medium mass nuclei, Phys. Rev. Lett. **123**, 092501 (2019).
[17] J. Rotureau, P. Danielewicz, G. Hagen, G. R. Jansen, and F. M. Nunes, Microscopic optical potentials for calcium isotopes, Phys. Rev. C **98**, 044625 (2018).
[18] J. Rotureau, P. Danielewicz, G. Hagen, F. M. Nunes, and T. Papenbrock, Optical potential from first principles, Phys. Rev. C **95**, 024315 (2017).
[19] N. K. Timofeyuk and R. C. Johnson, Nonlocality in deuteron stripping reactions, Phys. Rev. Lett. **110**, 112501 (2013).
[20] I. R. Afnan and F. J. D. Serduke, Off-shell effects in the three-nucleon bound state, Phys. Lett. B **44**, 143 (1973).
[21] A. W. Thomas and I. R. Afnan, Charge symmetry as a constraint on off-shell effects in the three-nucleon system, Phys. Lett. B **55**, 425 (1975).
[22] M. I. Haftel and F. Tabakin, Off-shell effects in nuclear matter, Phys. Rev. C **3**, 921 (1971).
[23] B. A. Watson, P. P. Singh, and R. E. Segel, Optical-model analysis of nucleon scattering from $1p$-shell nuclei between 10 and 50 MeV, Phys. Rev. **182**, 977 (1969).
[24] J. Lei and P. Descouvemont, Lagrange-mesh R -matrix method for inhomogeneous equations, Phys. Rev. C **102**, 014608 (2020).
[25] P. Descouvemont and D. Baye, The R -matrix theory, Rep. Prog. Phys. **73**, 036301 (2010).
[26] F. M. Nunes and A. Deltuva, Adiabatic approximation versus exact Faddeev method for (d, p) and (p, d) reactions, Phys. Rev. C **84**, 034607 (2011).

[27] F. M. Nunes, A. M. Mukhamedzhanov, C. C. Rosa, and B. Irgaziev, Insight into continuum couplings, Nucl. Phys. A **736**, 255 (2004).

[28] D. Y. Pang, N. K. Timofeyuk, R. C. Johnson, and J. A. Tostevin, Rapid convergence of the Weinberg expansion of the deuteron stripping amplitude, Phys. Rev. C **87**, 064613 (2013).

[29] J. Liu, J. Lei, and Z. Ren, Testing the validity of the surface approximation for reactions induced by weakly bound nuclei with a fully quantum-mechanical model, Phys. Rev. C **108**, 024606 (2023).

[30] T. L. Ma, B. Guo, Z. H. Li, Y. J. Li, D. Y. Pang, Y. L. Han, Y. P. Shen, J. Su, J. C. Liu, Q. W. Fan, Z. Y. Han, X. Y. Li, G. Lian, Y. Su, Y. B. Wang, S. Q. Yan, S. Zeng, and W. P. Liu, Precision measurement of the angular distribution for the ^{16}O(d, p) ^{17}O transfer reaction to the ground state of ^{17}O, Nucl. Phys. A **986**, 26 (2019).

[31] J. Lei and A. M. Moro, Reexamining closed-form formulae for inclusive breakup: Application to deuteron- and ^{6}Li-induced reactions, Phys. Rev. C **92**, 044616 (2015).

[32] M. Ichimura, N. Austern, and C. M. Vincent, Equivalence of post and prior sum rules for inclusive breakup reactions, Phys. Rev. C **32**, 431 (1985).

[33] M. S. Hussein and K. W. McVoy, Inclusive projectile fragmentation in the spectator model, Nucl. Phys. A **445**, 124 (1985).

[34] T. Udagawa and T. Tamura, Derivation of breakup-fusion cross sections from the optical theorem, Phys. Rev. C **24**, 1348 (1981).

[35] A. J. Koning and J. P. Delaroche, Local and global nucleon optical models from 1 keV to 200 MeV, Nucl. Phys. A **713**, 231 (2003).